

JGR Earth Surface

RESEARCH ARTICLE

10.1029/2021JF006204

Key Points:

- Vertical thaw can be explained through (vertical) conduction in both isolated and connected taliks
- Advection is needed in addition to conduction to describe observed thaw in flow-through taliks and lateral thaw rates adjacent to wetlands
- Deep subsurface temperatures provide evidence for thaw from below in permafrost features bordering fens

Supporting Information:

Supporting Information may be found in the online version of this article.

Correspondence to:

É. G. Devoie,
egdevoie@uwaterloo.ca





Citation:

Devoie, É. G., Craig, J. R., Dominico, M., Carpino, O., Connon, R. F., Rudy, A. C. A., & Quinton, W. L. (2021). Mechanisms of discontinuous permafrost thaw in peatlands. *Journal of Geophysical Research: Earth Surface*, 126, e2021JF006204. <https://doi.org/10.1029/2021JF006204>

Received 6 APR 2021

Accepted 4 OCT 2021

Mechanisms of Discontinuous Permafrost Thaw in Peatlands

Élise G. Devoie¹ , James R. Craig¹ , Mason Dominico² , Olivia Carpino² , Ryan F. Connon³, Ashley C. A. Rudy⁴, and William L. Quinton²

¹Department of Civil and Environmental Engineering, University of Waterloo, Waterloo, ON, Canada, ²Cold Regions Research Centre, Wilfrid Laurier University, Waterloo, ON, Canada, ³Environment and Natural Resources, Government of the Northwest Territories, Yellowknife, NT, Canada, ⁴Northwest Territories Geological Survey, Government of the Northwest Territories, Yellowknife, NT, Canada

Abstract Climate warming in discontinuous permafrost peatlands is causing permafrost loss and changes in ecosystem dynamics at an unprecedented rate. Though rates of permafrost loss and landscape change have been widely documented based on remote sensing and field measurements, the local mechanisms of permafrost degradation remain under-studied. These mechanisms were explored using data collected over three decades of research in the Scotty Creek study basin in the southern Northwest Territories of Canada. The data, when compared to numerical modeling results, demonstrated that vertical heat conduction accounts for most vertical permafrost degradation, while advective heat transfer drives thaw in features which are subject to seasonal flows. It was found that heat advection was necessary to describe lateral thaw rates of up to 115 cm annually, which are an order of magnitude greater than vertical thaw rates, which average 10 cm annually. Thaw from below, driven either by the geothermal gradient or groundwater flow, may account for up to 10 cm of permafrost thaw annually. The hydrologic, thermodynamic and geophysical function of taliks in different parts of the landscape were considered in light of the data collected at the field site and surrounding area. This analysis is supported through the use of ERT data detailing the subsurface permafrost structure. This understanding of local thaw mechanisms and trajectory is an important first step in being able to predict distributed permafrost thaw in peatlands.

Plain Language Summary Permafrost (ground frozen for two or more consecutive years) in northern wetlands with is thawing quickly due to climate warming. Though this thaw is widely documented, the specific mechanisms responsible for the loss of permafrost in the landscape are under-studied. This work presents data collected at the Scotty Creek field site in the southern Northwest Territories of Canada alongside modeling results to describe the mechanisms for thaw in each part of the landscape. At this site, permafrost is surrounded by permafrost-free wetlands. It is found that permafrost loss from the ground surface downward is mostly dependent on the amount of energy received at the ground surface. However, if two wetlands are connected by a channel, flow through this feature contributes to thaw. When considering permafrost loss at the edge of permafrost bodies, energy transported with flow is necessary. Thaw from the base of permafrost bodies is driven by the heat from the Earth's core (geothermal gradient). Some or all of these thaw mechanisms may be acting together to drive the rapid thaw observed at this study site.

1. Introduction

Permafrost thaw is driven by climate warming, which is amplified in arctic and sub-arctic regions (Pörtner et al., 2019). Thaw rates in discontinuous and sporadic permafrost zones are strongly dependent on land cover types, where ecosystem-protected permafrost beneath organic soils tends to persist even after the climate is unfavorable for permafrost development (Bonnaventure & Lamoureux, 2013). In discontinuous permafrost peatlands, it has been demonstrated that thaw rates over the last five decades have led to significant permafrost losses, especially lateral loss adjacent to wetlands (Chasmer et al., 2011). Similar patterns of permafrost loss linked with water movement and hydrologic change have been noted in the Yukon Flats and in northern Sweden (Sjöberg et al., 2016; Walvoord & Kurylyk, 2016; Walvoord et al., 2019). It has also been determined that subsurface heterogeneity in soils, soil moisture, and soil properties have led to variations in observed thaw rates, and have explained some of the patterns of talik formation (Amiri & Craig, 2019).

Recent work has identified supra-permafrost taliks as important thaw features (O'Neill et al., 2020). In this work, taliks refer to perennially thawed layers overlaying permafrost, and it is thought that their formation is often the first stage of permafrost degradation in permafrost peatland environments (Devoie et al., 2019).

Two mechanisms for heat transfer driving thaw are considered: conduction and advection. In cases where water movement is not observed in the thawed or thawing soils, it is proposed that conduction is the dominant mechanism for heat transfer. Conduction is governed by Fourier's law (Fourier, 1878):

$$q = -k \frac{dT}{dz} \quad (1)$$

where q [W/m^2] refers to the conductive heat flux, k [$\text{W/m}^\circ\text{C}$] is the thermal conductivity of the media, T refers to the temperature [$^\circ\text{C}$] and z is the vertical depth [m]. Much of the heterogeneity in thaw arises from heterogeneity in thermal conductivity, k , which is a function not only of the soil properties, which are often spatially variable, but also depends strongly on soil moisture content and phase. Soil moisture, and its partitioning as water or ice is temporally variable and controlled by topography, vegetation and soil properties (Hayashi et al., 2007; Wright et al., 2009).

The second mechanism driving thaw is advective heat flux, the term used to describe advection-enhanced conduction in which flowing water strengthens the thermal gradient in the direction perpendicular to the flow. The advective heat flux as described here may be considered using the following equation, which describes heat transfer q [W/m^2] from a moving fluid with velocity v [m/s], density ρ [kg/m^3], specific heat c_p [J/kgK], and temperature difference ΔT between the inflowing and outflowing water:

$$q = v c_p \rho \Delta T \quad (2)$$

In the 1-D case of vertical thaw, this advective movement of energy is taken to be in the x - y plane while thaw occurs in the z direction, as permafrost is often assumed to be impermeable, precluding (true) vertical advection (Quinton et al., 2003). Advection is only a driver of vertical permafrost thaw when taliks provide a flow conduit between wetlands with different hydraulic heads, driving flow with a velocity v over the surface of the frost table (Devoie et al., 2019). This is relatively rare in discontinuous permafrost, though it has been observed in cascading collapse scar wetland series documented at the Scotty Creek study basin in the southern Northwest Territories (R. F. Connon et al., 2015).

Advection is much more likely to play a dominant role in lateral permafrost thaw rather than vertical thaw, which is reported to account for a significant fraction of permafrost loss in discontinuous permafrost landscapes (McClymont et al., 2013). This thaw occurs preferentially along the boundary between wetlands (permafrost-free) and the adjacent permafrost terrain, where the thermal energy stored in wetlands establishes a perennial thermal gradient from the wetland to the permafrost. Water moving horizontally adjacent to permafrost acts to maintain the thermal gradient between the permafrost body and the thawed wetland.

Talik formation often leads to local ground surface subsidence, including areas of moisture convergence, especially in areas where the water table is already near the ground surface. Subsidence increases the soil moisture content, and consequently the thermal conductivity of the soil, resulting in a positive feedback (R. Connon et al., 2018). This positive feedback is only strengthened by the vertical thermal gradient which is highly dependent on talik presence. In the summer, the thermal gradient is directed downwards, conducting heat deeper into the soil, while in the winter months the permafrost is decoupled from the cold atmosphere by the talik, and is unable to lose heat and continues to be subjected to a positive thermal gradient (R. Connon et al., 2018). Talik formation is therefore considered a tipping point in the process of permafrost thaw (Devoie et al., 2019). In some cases, the thermal gradient between the permafrost and the talik is nearly nonexistent because the latent heat of phase change between liquid water and ice is almost two orders of magnitude greater than the heat capacity of water. During phase change, energy transfer can occur isothermally, leaving the temperature of the talik features near the freezing point year-round.

Though permafrost degradation is likely driven by a combination of vertical and lateral conduction and advection, the relative importance of each of these processes is unclear in the landcover types comprising the peatland-dominated southern margin of thawing discontinuous permafrost. The aim of this work is to characterize the dominant mechanisms for permafrost thaw and quantify their relative importance in peatland dominated terrains with discontinuous permafrost. A combination of field observations and modeling

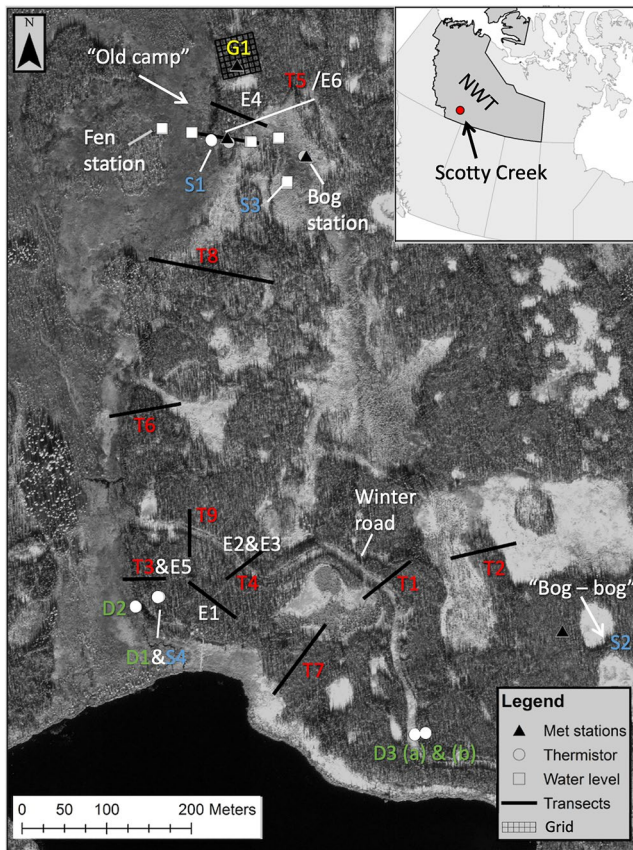


Figure 1. Location of field site inset on aerial imagery of study site. Frost table transects (T) and locations of meteorological stations (named), water level records (white squares), ERT transects (E) and deep (D) and shallow (S) thermistors indicated.

studies were completed to identify drivers for permafrost thaw across the landscape to improve the representation of thaw processes in future models of land cover evolution and hydrology.

2. Study Site

This study was undertaken at the Scotty Creek study site (SC) located approximately 70 km south of Fort Simpson in the Northwest Territories, Canada (Quinton et al., 2017) as seen in Figure 1. This site was selected because it has a long data record with instrumentation documenting the formation and evolution of taliks. It is representative of peatland head-water regions of the Mackenzie and Liard rivers (O. Carpino et al., 2021).

The SC study basin was established in 1999, and is an ideal location for the study of permafrost degradation because it includes permafrost in different stages of degradation including stable permafrost, isolated and connected taliks, and permafrost-free wetlands (R. Connon et al., 2018). The peat deposit in this study site ranges from 2 to 8 m in thickness, and overlays clay, silt/clay, and low-permeability glacial till (Quinton et al., 2019). High permeability near-surface peat soils drain readily when the water table is below the ground surface, leaving a relatively dry insulating surface peat layer that preserves permafrost underlying peat plateaux (Quinton et al., 2009). Though insulated from the high summer temperatures, the permafrost in this discontinuous permafrost site is warm (at or just below 0°C), and a significant portion of it is within the zero curtain (undergoing phase change). Peat plateaux are elevated above the surrounding permafrost-free wetlands that have undergone subsidence due to permafrost thaw and loss of pore ice (Quinton et al., 2009). The ground cover of peat plateaux is dominated by non-transpiring lichens and mosses which limits water loss from this vegetation to soil evaporation and water wicked by wet ground cover, while sparse vascular ground cover persists in some areas, with a canopy of black spruce. These plateaux are surrounded by two wetland types that dominate the landscape, collapse scar wetlands and channel fens. Collapse scar wetlands act mainly as water storage features, and are *Sphagnum*-dominated clearings (Quinton et al., 2009). Though sometimes referred to as bogs, collapse scar wetlands do not fit the true ombrotrophic definition of a bog as they may be ephemerally connected to other wetlands through narrow channels (R. F. Connon et al., 2015). They receive both direct precipitation and lateral inputs from surrounding plateaux. Channel fens separate the plateau-collapse scar wetland complexes, which are composed of plateaux and collapse scar wetlands. Though they have a low hydraulic gradient, fens are the routing feature in this flat, high-storage landscape (Gordon et al., 2016). Fens are sedge-dominated, and contain hummocky terrain that supports larch (*Larix laricina*) stands. These are relatively sparse in comparison to the black spruce on plateaux. The water table is generally found up to 0.2 m below the ground surface in the wetlands while it remains between 0.5 and 0.7 m below the ground surface on plateaux at the end of summer when the active layer is fully developed. This is also the maximal depth of the active layer observed in this site (R. Connon et al., 2018).

3. Methods

A combination of field data collection at SC and modeling was used to assess the mechanisms for permafrost thaw in various parts of the discontinuous permafrost peatlands landscape at SC.

3.1. Field Site Selection

Field sites at SC were selected to document permafrost degradation in different talik and thaw features of the landscape, classified into the six types depicted in Figure 2. The first four features are a progression from

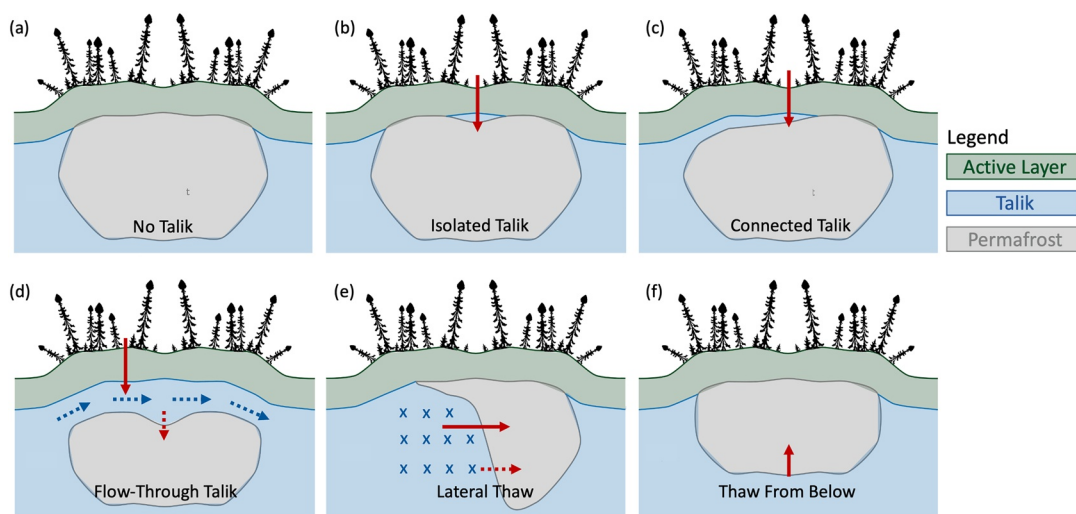


Figure 2. Different talik features observed at Scotty Creek. Perennially thawed areas and taliks are shown in blue (note this refers only to thermal state and not water table position). Different types of heat flux responsible for thaw in various taliks shown in red. Solid red arrows indicate conduction, dashed red arrows indicate advection-enhanced thaw. Dashed blue arrows indicate water flow, and blue crosses indicate flow into the page. Conceptual diagram not to scale.

(a) the “no talik” condition, where the active layer is fully frozen in the winter, to (d) the “flow-through talik” condition, which permits lateral flow assuming the left wetland has a higher water table position than the right. Panel (e) depicts lateral thaw with advection (into the page), and (f) highlights the potential for permafrost degradation from below. Both (e and f) may occur simultaneously with vertical talik formation depicted in (b–d). Note that taliks here refer both to the confined regions sandwiched between the active layer and the top of the permafrost body, as well as permafrost-free wetlands abutting and surrounded by permafrost bodies.

3.2. Frost Table Measurements

Frost table measurements were taken using a frost probe along nine transects (T1–T9) and in a grid (G1), established in 2011, which can be seen in Figure 1. A graduated steel rod was inserted into the ground until the point of refusal. This measurement was taken annually at the end of the thawing season (typically late August or early September), and indicates the maximal thaw extent. Change in the frost table position year-to-year along these transects provided a measure of vertical thaw, while lateral thaw was established through detailed measurement of the change year-to-year in the endpoints of the permafrost bodies. The graduated steel rod was also used to probe the exact location of the edge of the permafrost feature where it transitions to a wetland.

3.3. Temperature and Heat Flux Measurements

In addition to these measurements, temperature profiles were established at several sites - three deep thermistor profiles (RBR-limited: 10 sensor temperature loggers) were installed to measure subsurface temperature at 1 m intervals to a depth of 6–10 m (D1–D3 (a and b) shown in Figure 1). These sensors were located on a plateau adjacent to a linear disturbance on the landscape (winter road), and on the border of a fen. Shallower temperature data were collected at three additional sites: one in an ephemeral channel between two wetlands (S1 and S2 similar to panel (d) of Figure 2 which is termed a “flow-through talik”), one on a plateau (S4), and one in a collapse scar wetland (S3). These profiles were measured using Campbell Scientific CS 107 or CS 109 thermistors connected to Campbell Scientific CR1000 or CR10X loggers, with measurement intervals of 5–15 cm.

These data were augmented by Hoskin Scientific ground heat flux plates installed at an isolated talik site (black triangle located G1 in grid in Figure 1). Ground heat flux plates were installed to quantify the

cumulative vertical ground heat flux (Q_g [J/m²]) annually. This energy is converted to cm of permafrost thaw, Δz , using:

$$\Delta z = \frac{Q_g}{(\eta - S_{res})\rho_i\lambda_f} \quad (3)$$

where the porosity of peat is (η), the latent heat of fusion of water is (λ_f [J/kg]), S_{res} is the residual liquid water content after freezing, and ρ_i [kg/m³] is the density of ice.

3.4. Hydrologic Measurements

HOB0 U20L pressure transducers were used to measure hydraulic gradients. These sensors were installed in slotted wells situated in the center of collapse scar wetland features, and logged pressure at half-hour intervals. This pressure record was corrected to account for atmospheric pressure before being converted to an equivalent depth of water. The hydraulic gradients in this landscape are very low due to the flat topography, and the use of piezometers to detect lateral flow was not possible. As an alternative, EnvironFlux passive flux meters were used to establish flux through low-gradient talik connections. These sorbent-packed wells were installed in flow-through taliks for one season to determine the cumulative water flux through the talik connection using the desorption of solutes (Devoie et al., 2020). The location of these field sites, S1 and S2, is indicated in Figure 1, alongside subsurface soil temperature profiles. The observed seasonal mass flow data (\dot{m} [kg/s]) and the specific heat of water were used with the mean seasonal subsurface temperatures ($T(z)$) over the depth of the profile assumed to influence the permafrost table, h , to quantify the energy available to drive thaw:

$$\int_0^{365d} \int_0^h \frac{\dot{m} C_p \Delta T(z)}{h} dz dt = \eta \rho \lambda \Delta z \Delta x \cdot 1m \quad (4)$$

The depth h [m] was assumed to be one half of the depth of the talik in the winter - the bottom half of this feature would affect the underlying permafrost while the top half would interact with the active layer. In the summer, h was taken to be the full thawed depth of the thawed profile. The right hand side of Equation (4) represents the mean loss of permafrost along the transect, for a unit transect width. In this relation, η [m³/m³] represents the soil porosity, ρ [kg/m³] is the soil density, λ [J/kg] is the latent heat of fusion of water, Δx [m] represents the length of the transect, and Δz [m] is the resulting vertical loss of permafrost.

3.5. ERT Data Collection and Processing

Electrical resistivity tomography (ERT) surveys were collected in late August of 2018 and 2019 at SC when thaw depths are thought to be at their maxima (McClymont et al., 2013). The large contrast between the resistivity of frozen and unfrozen water make ERT a useful technique to delimit subsurface permafrost, especially in high-porosity soils near saturation such as those observed at SC (Kneisel et al., 2008). Surveys were collected with a SuperSting R8 (AGI, Austin, Texas, USA) and a 56-electrode cable at an electrode spacing of 1 m. Both Wenner and dipole-dipole strong gradient (DDSG) arrays were collected at each site. The Wenner array provides a strong signal and increased ability to resolve vertical structures where as the DDSG provides increased resolution (Sjöberg et al., 2016). Following each survey frost table depths were measured using a 1.5 m graduated steel probe along the transect at 1 m intervals to validate the location of the top of the permafrost table (if present). The location of these transects is shown as E1–E6 in Figure 1.

Raw ERT data were processed using AGI Earthimager 2D version 2.4.4 (Build 649), an iterative-based two-dimensional inversion software. Prior to inversion both the Wenner and DDSG array were merged into a single file to create a mixed array data set for improved resolution. The robust inversion method was chosen for the inversion process as it performs best when sharp changes in resistivity are expected, such as between permafrost and thawed ground (Loke et al., 2003; McClymont et al., 2013). The inversion process continued until the RMS error dropped below 5%, or the fifth iteration (Sjöberg et al., 2016; Way et al., 2018). To correct for topography, the start and end locations of each transect were recorded with a handheld GPS (Garmin inReach Explorer +). Using the GPS coordinates, the profiles were then corrected for topography using a 1-m digital elevation model (Lewkowicz et al., 2011).

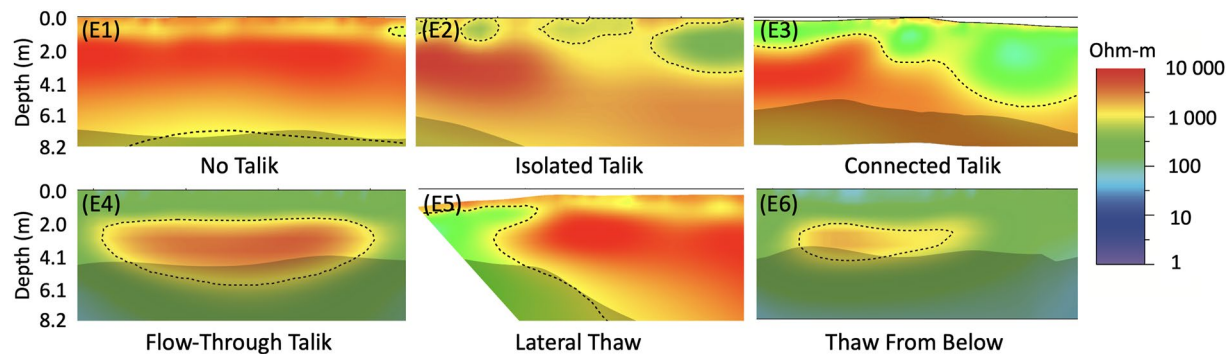


Figure 3. Electrical resistivity tomography data collected at the Scotty Creek, classified according to the six established permafrost configurations from Figure 2, and E1 through E6 on the site map. High resistivity (red) indicates frozen (or dry) soil, while low resistivity (blue) indicates thawed and saturated soil. Note the gray shaded (not on color legend) area at the base of the profiles indicates increased measurement uncertainty, while dotted lines are inferred boundary between frozen and thawed soil (taken to be 1,000 Ω).

3.6. Modeling Methods

The numerical interface model of freeze thaw presented in Devoie and Craig (2020) was used to test hypotheses regarding the interpretation of field measurements. This is a semi-analytical model where the position of one or more freeze/thaw interfaces is tracked using a superposition of analytical solutions to the heat equation. The movement of water in the subsurface is assumed to be in an equilibrium state, and an energy conservation approach is taken in each element which is allowed to change size as the interface moves. Readers are directed toward Devoie and Craig (2020) for model details and benchmarking. This 1-D model was used without advection or unsaturated flow to establish if conduction alone was sufficient to reproduce observed thaw rates for steady moisture content distributions. A range of simulations were run for each talik configuration from Figure 2 by sampling the initial talik thickness, soil moisture and thermal boundary conditions from an ensemble of boundary and initial conditions bootstrapped from observed data collected at the SC. Talik thickness was sampled from a distribution with mean of 40 cm and standard deviation of 15 cm. The ensemble of thermal boundary conditions was generated using a seasonal auto-regressive integrated moving average (SARIMA) analysis, with input temperatures collected at sites with no talik (S4) with an isolated talik (S1) and one with a connected talik (S2) (Hipel & McLeod, 1994).

For simulations of a soil profile with no talik, or an isolated talik, the water table was fixed at a depth of 0.5 m below the soil surface while in talik conditions, a fully saturated soil profile was assumed based on observations in the field. Model initial conditions were consistent with the permafrost configuration. In the case of an isolated talik, this resembles the center of the “isolated talik” case in Figure 2b, while the connected talik simulations are arranged as panel (c) of this figure, where the top of the talik feature is 0.5 m below the ground surface. In the simulations, a uniform soil temperature of -0.1°C was assigned outside of a talik layer, while the talik was initialized with temperature of 0.1°C . Soil thermal properties were drawn from peat properties reported at the SC and were compared to data in literature to obtain a porosity of 0.8, a bulk saturated (thawed) thermal conductivity of $0.53 \text{ W/m}^{\circ}\text{C}$ and heat capacity of $3,472 \text{ J/kg}^{\circ}\text{C}$ (Price et al., 2005).

4. Results

The conceptual diagrams (Figure 2) of different talik types found at SC are supported by ERT data measured at transects E1–E6 (Figure 3). Note the similarities in ice configurations between this theoretical framework and data collected in the field. In Figure 3 we note that at the depth of about 8 m there is a transition from peat to silty clay mineral sediment with different dielectric properties, where the measured profile ends. High resistivity generally indicates frozen soil, but in the near-surface can also describe unsaturated thawed soil as in panels (E1), (E2), and (E5) of Figure 3. Note that panels (E4) and (E6) are only separated by 20 m, and the change in total depth of the permafrost is therefore unlikely due to differences in subsurface composition as mineral soil is found at a depth of more than 8 m in this area of the study basin, and is rather likely

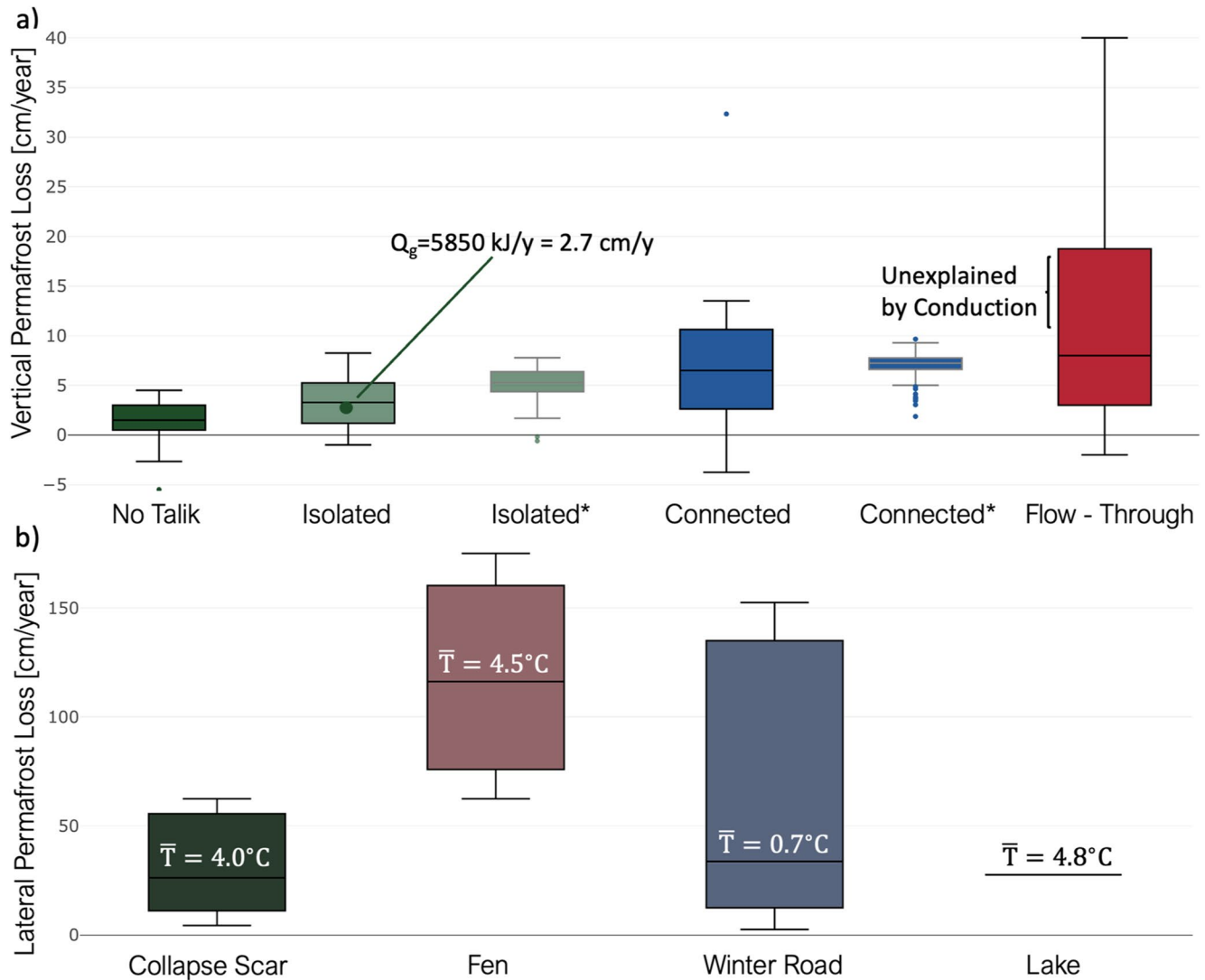


Figure 4. (a) Vertical permafrost degradation rates in talik types (a–d) from Figure 2, from data measured between 2011 and 2020 and modeled (indicated by an *) using vertical conduction alone for the isolated talik and connected talik cases. Green point indicates computed thaw based on ground heat flux in 2011. Modeled data is not presented for the flow-through talik case as it is identical to the connected talik case in the absence of horizontal flows. (b) Measured lateral permafrost degradation rates adjacent to all wetland types, noting that the winter road traverses both collapse scar wetland and fen features, while supporting flow and permafrost loss in the disturbance itself.

due to thaw from below, as will be discussed in Section 5.3. Areas shaded in gray have higher uncertainty due to low electrode sensitivity, and indicate areas which merit further investigation.

4.1. Vertical Thaw

Vertical and lateral permafrost thaw rates were quantified using manual frost probing, presented in Figure 4. These field data indicate widespread vertical permafrost loss, including active layer thickening on average 2 cm/year in areas without taliks. Where isolated taliks were present, data collected from ground heat flux plates amounted to 2.7 cm/year of thaw (green circle in Figure 4 - isolated). This aligns well with the observed mean permafrost degradation rate of 3.4 cm/year. In addition, simulations generated using the interface model described in Section 3.6 of an unsaturated soil column forced with boundary and initial conditions sampled from field data collected in four isolated talik sites compare favorably with the observed thaw rates (Figure 4 - isolated*). In connected taliks, the observed mean thaw is somewhat higher than that observed in isolated taliks and the variance in observed thaw rates is also significantly greater (Figure 4 -

connected). The vertical conduction-only model is again used with boundary and initial conditions extrapolated from field data at representative sites (as described in Section 3.6) to reproduce the mean observed thaw rate as seen in Figure 4 - connected*. However, the model does not reproduce the observed spread in data. An even wider spread in data is seen in Flow-through taliks. These are taliks confined between the active layer and the permafrost table, but with connections to more than one wetland. Comparing this with the connected model case in Figure 4a, the upper tails of permafrost degradation rates shown by the bracket (approximately 30% of measured taliks) in flow-through taliks cannot be explained by conduction alone. As calculated using Equation 4, for data collected at SC, advection-driven permafrost loss is expected to fall between 0.6 and 8 cm of thaw annually, based of inter-annual and inter-site variations in subsurface flow. This range can account for the unexplained variability in thaw and high thaw rates observed in flow-through taliks in Figure 4 - (flow-through), and suggests that the combination of vertical conduction and advection are both needed to provide the energy necessary to describe the observed thaw in flow-through taliks.

4.2. Lateral Thaw

Lateral thaw observed in the discontinuous permafrost landscape occurs approximately one order of magnitude more quickly than vertical thaw, as seen by comparing panels (a and b) of Figure 4. Given that both collapse scar wetlands and fens have waterlogged “moat” features that run along their peripheries, the thermal conductivity is very similar in both features. If the thaw could be explained through conduction alone, Fourier’s law of conduction, (Equation 1 when applied in the x direction), would imply that the rate of permafrost degradation is proportional to the temperature gradient, and thus also to the temperature of the adjacent wetland, assuming that thaw occurs near 0 °C. The temperature gradient established between a fen and a plateau would be expected to be more than three times that observed between collapse scar wetlands and plateaux since the observed thaw rate is about 115 cm/year near fens compared to about 30 cm/year near collapse scar wetlands. This is not the case, as the average collapse scar wetland temperature at a depth of 90 cm is 3.95 °C with an annual variance of ± 6.1 °C (S3), while the average fen temperature at 100 cm is 4.45 ± 5.6 °C (Fen station). This points to a potential for significant contribution of advection-driven thaw in lateral permafrost loss.

4.3. Thaw From Below

In addition to vertical thaw from above, and lateral thaw, the potential for permafrost degradation from below should also be considered. Evidence for thaw from below takes the form of temperature gradient reversals where the temperature at depth exceeds that near the surface as seen in Figure 5b. This may be caused by the geothermal gradient - reported to be approximately 0.08 W/m² at a depth of 50 m in this landscape (McClymont et al., 2013); but may also be partially driven by subsurface flows. Evidence for subsurface water movement is provided by deep thermistor profiles, as shown in Figure 5. More rapid and dynamic permafrost loss at depth near to the fen as compared to the stationary data from the winter road are shown in panel (c) of Figure 5 as a shift in the trumpet plot. This is thought to be driven in part by the warm temperatures at depth over winter in panel (b) of this figure.

4.4. Nonstationarity

Over the course of the three decades of data recorded at SC, and even the five years of data collection that contributed directly to this study, significant changes in the landscape were observed. For instance, a flow-through talik was found and instrumented in 2016 (S2). In Figure 6b, the subsurface temperature profile at this site was initially similar to that observed on a stable peat plateau (indicated in dark blue; S4). However, by 2020 we observe that the temperature profile is now much more similar to the collapse scar wetland condition (red - S3). In panel (a) of this figure, a time series of this thermistor data is presented where it is clear that the summer warming is reaching greater depths year over year.

This extremely rapid transition is not unique to this particular site as similar results are observed in a flow-through talik that was instrumented much earlier in its formation (S1). Figure 7 shows the degradation of this plateau separating two wetlands over the last two decades (along with the shorter time series drawn from the site instrumented in 2016: “Bog-Bog”).

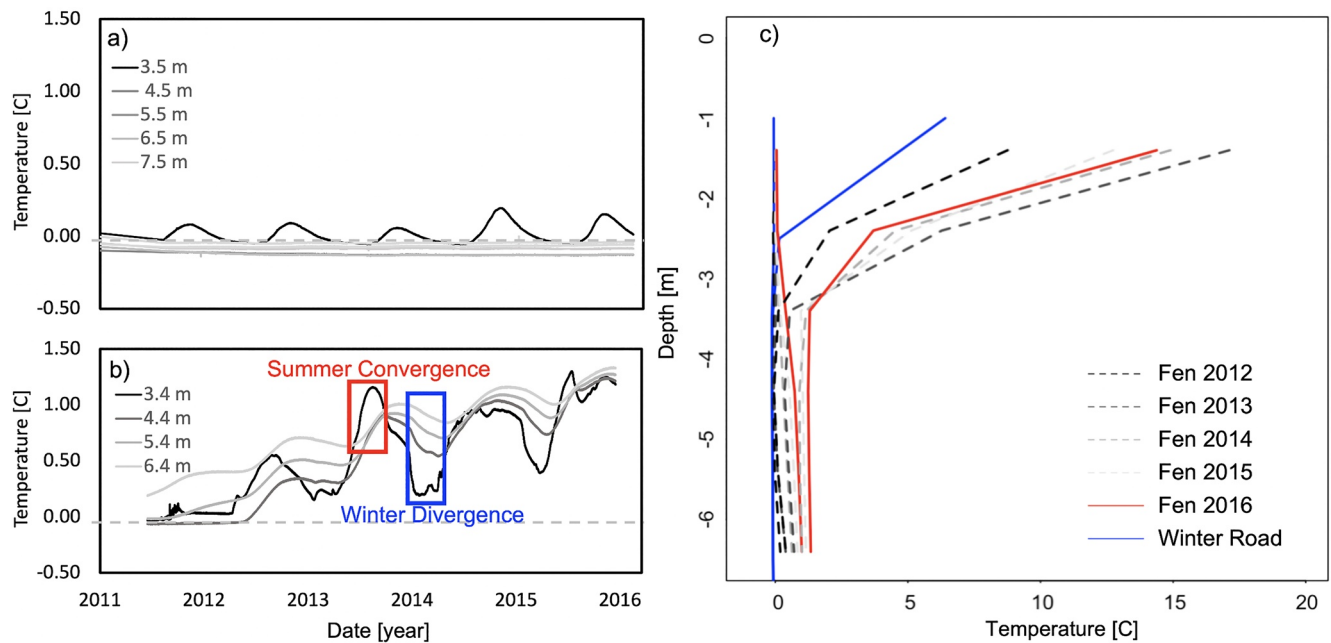


Figure 5. Measured subsurface temperature below (a) a plateau and near (b) a fen at multiple depths. Annual maximum and minimum data for the fen is represented in a trumpet plot, and compared to the stationary data (no detectable change at depth over the period of record) for the winter road (blue) in (c).

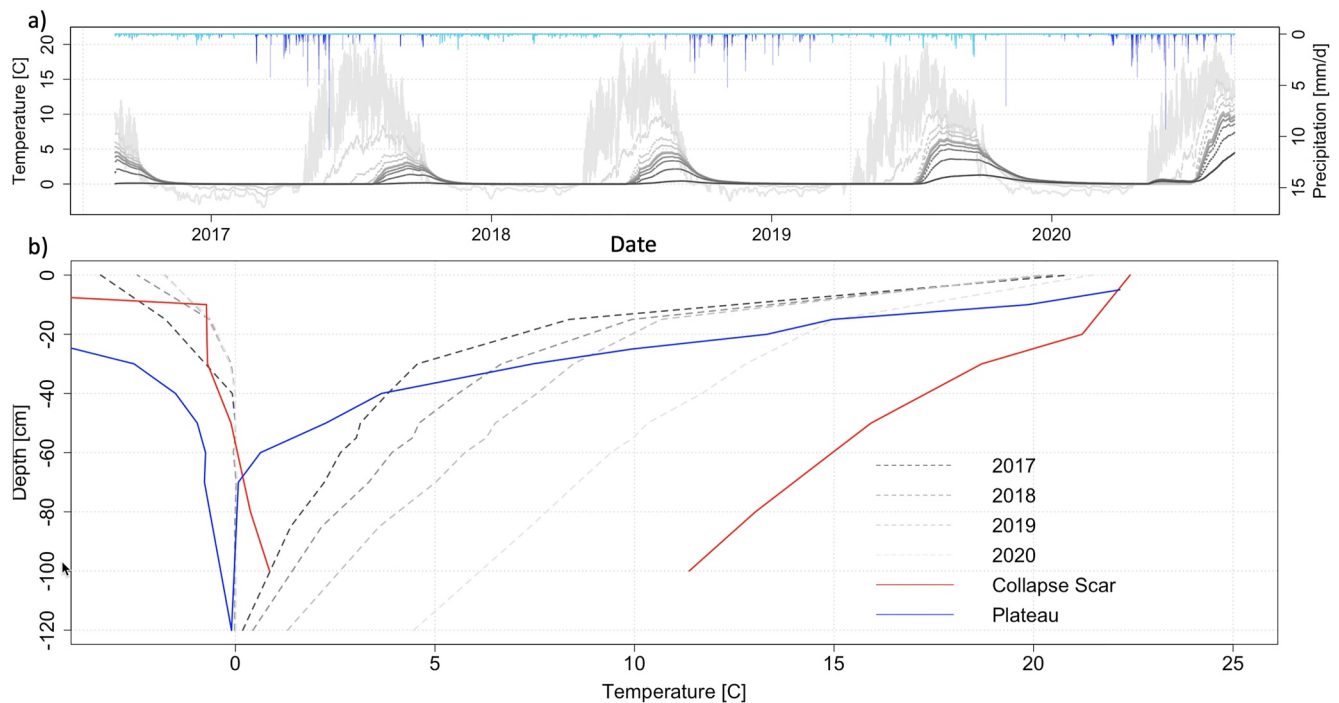


Figure 6. (a) Temperature profile of talik with advection between two collapse scar wetlands. Air temperature shown in light gray and subsurface temperatures shading darker with depth from the surface to 2 m with approximately 10 cm spacing. Note the increasing depth of active layer warming in the summer and the isothermal conditions over winter indicating incomplete refreeze. Precipitation shown along the top axis, where light blue is snow and dark blue is rain. (b) Trumpet plot of talik development with advection between two collapse scar wetlands (bog-bog in Figure 1). End members of permafrost warming are shown as plateau (blue) and collapse scar wetland (red) over the period from 2014–2019.

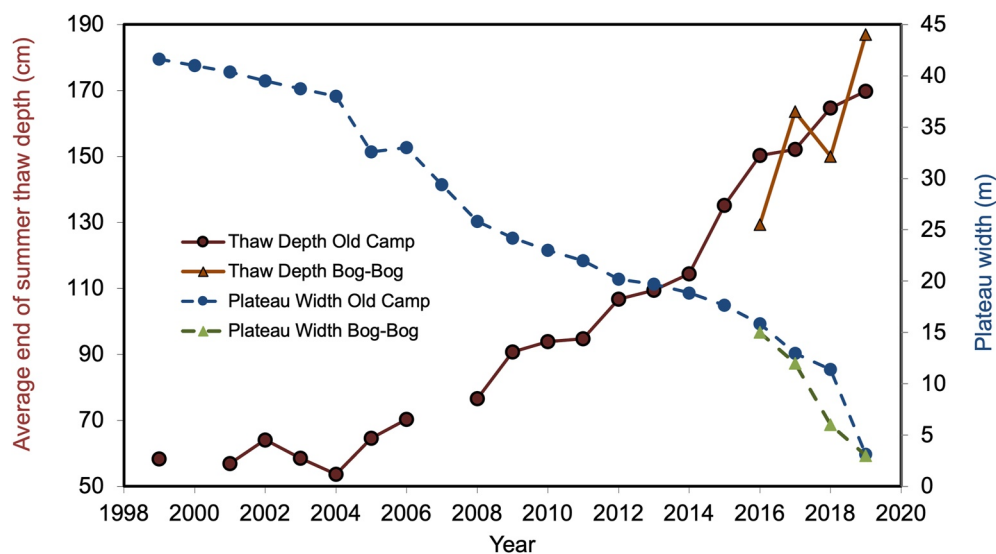


Figure 7. Simultaneous vertical and lateral permafrost thaw observed at two sites in Scotty Creek. There are two notable turning points: when the thaw depth exceeds about 70 cm, the rate of permafrost degradation increases, and again when the thaw depth reaches about 110 cm and the width is 15–20 m, there is an inflection point. Both flow-through talik connections are indicated in Figure 1 by mane (“Bog-Bog” and “Old Camp”).

5. Discussion

The four possible heat transfer mechanisms leading to permafrost thaw are: (a) vertical conduction, (b) advection through a talik feature, (c) lateral conduction and (d) lateral advection. In both advective cases, thaw itself is conduction driven but the temperature gradient at the permafrost surface is enhanced by flow adjacent to the permafrost surface. This term could alternatively be interpreted as a convective flux to the permafrost, but horizontal advection is used here for consistency with work presented in Devoie et al. (2019). To understand the heterogeneity in observed thaw rates at SC, the landscape is classified into four categories described in relation to Figure 2, and the drivers of permafrost thaw (1 through 4) are considered in each of these categories.

5.1. Vertical Thaw

5.1.1. Category 1: No Talik

The first permafrost category describes the case in which there is no talik present (Figure 2a). In this case the active layer fully freezes from the soil surface to the permafrost table overwinter. Without liquid water available to drive advection-enhanced thaw, the only mechanism for heat transfer is vertical conduction. In a stable climate, this condition should be non-evolving, such that the active layer completely re-freezes every winter. These conditions were historically present at this site and led to the initial development of permafrost. However, active layer thickening is observed in the field data collected at SC. This is a process reported by Shiklomanov et al. (2012), in which active layers deepen due to increases in net ground heat flux. Active layer thickening can only persist until the depth of thaw reaches the maximal depth of refreeze. After this point, insufficient heat is lost from the ground over the winter to balance the positive net radiation over the summer. This is especially true of profiles in which thaw-driven subsidence has led to increased moisture content in the near-surface soil (increasing thermal conductivity), browning of the lichen ground cover (decreasing albedo), and the formation of a depression in which snow can accumulate (insulating the soil over winter). Frost table data collected at the SC site documenting the change in permafrost conditions provides evidence for this process, where taliks increased in prevalence from 8% to 33% between 2011 and 2016 (R. Connon et al., 2018).

5.1.2. Category 2: Isolated Talik

Once a talik is formed, a perennially thawed soil layer exists between the active layer and the permafrost table (Figure 2b). Here the term isolated indicates the talik is surrounded on all sides and below by permafrost, but is overlain by an active layer. The talik effectively decouples the permafrost below it from the atmosphere in the winter because it is above the freezing point, thus preventing the permafrost from losing energy vertically to the soil surface, and resulting in permafrost loss year-round (R. Connon et al., 2018). In the case of an isolated talik surrounded on all sides by permafrost, it is hypothesized that permafrost loss can be attributed to vertical conduction alone, and that other heat transfer mechanisms are negligible. Lateral conduction is unlikely due to the lack of lateral thermal gradients, and the scarcity of water movement in isolated taliks means only a small energy input can be expected from summer precipitation events and advection is unlikely. We examine this hypothesis by comparing the observed rate of permafrost degradation calculated from (a) measured ground heat flux, and (b) simulated heat transfer from the interface model. This conduction-only model over-estimates the observed thaw, indicating that vertical conduction is sufficient to describe permafrost degradation occurring in isolated taliks. This does not preclude other processes from contributing to thaw, only that this single process is sufficient to account for this thaw, and the likelihood is therefore high that the influence of other processes is negligible.

5.1.3. Category 3: Connected Talik

Taliks are also frequently found adjacent and connected to wetlands (Figure 2c). The observed increase in thaw rate in these taliks as compared to isolated ones may be partially explained by a mean increase in incoming radiation near wetlands, where the canopy-free wetlands allow for more radiation to reach the surrounding permafrost bodies, especially on south-facing edges and during periods with low sun angles. These differences in canopy cover and incoming radiation to permafrost adjacent to different wetlands may explain the increased variance in observed thaw rates in connected taliks as compared with modeled results based on subsurface temperatures measured at S1 and in G1 in Figure 1. It may also point to a need to consider advection in certain wetlands where water is moving sufficiently to convey heat to the connected talik. While every effort was made to measure the frost table in identical locations year to year, it is likely that these measurements were made in slightly different locations around each flagged point (i.e., within a 5 cm radius). The high local variability in frost table position (changing up to 5 cm vertically in a 5 cm radius) likely led to some error in measurement. As discussed in (Ackley et al., 2021), the local variance in frost table topography is high, both in disturbed areas such as burns or flow-through taliks and in undisturbed ones. Additionally, changes to ground cover and establishment of mosses may have altered the heat flux conditions in some sites, leading to limited permafrost recovery. The model results indicate that vertical conduction alone is sufficient to explain the mean thaw rate observed in these connected taliks, and is therefore likely the dominant thaw mechanism, as it was for the isolated case, but the high variability in thaw indicates that this process is either highly sensitive to landscape heterogeneity, or other processes play a role in the permafrost degradation.

5.1.4. Category 4: Flow-Through Talik

The landscape features in which the most rapid vertical permafrost degradation is observed are termed flow-through taliks (Figure 2d). If the connected wetlands differ in hydraulic head, a gradient is established across the talik, driving lateral water flow over the permafrost surface. Depending on the temperature of the wetlands, this flow can transport warmer water across the permafrost table which can enhance vertical permafrost degradation through advection year-round, even in winter when the air temperature is below the freezing point, as calculated using Equation 4. In more than 30% of the sites, advective heat transfer is required to reproduce the observed thaw. Figure 4 also shows a large variance in observed thaw rates in flow-through talik features, which can be attributed in part to the wide variance in measured flow rates in connected talik features, and in part to the spatial variability and change in vegetation discussed above. Heterogeneity in subsurface soil and flow patterns not included in the 1-D model would also be expected to contribute to the variability in observed thaw rates. It is not expected that density effects would play a role in defining the vertical thermal gradient in these or other talik features for two reasons: first, the change in density of water between the freezing point and 5 °C is minimal as compared to the pycnocline at higher temperatures. Second, the porous structure of peat is not conducive to the circulation of water due to its dual porosity (Rezanezhad et al., 2012), especially as compared to a body of water undergoing lake turnover.

This is supported by the temperature profiles reported in Figure 6a in which there is no evidence of isothermal conditions at 4 °C, or any reversals of the thermal gradient other than those seasonally driven by the soil surface temperature.

5.2. Lateral Thaw

Instead of being driven by summer temperature gradients from above, lateral thaw occurs year-round adjacent to permafrost-free wetlands. As in the vertical case, both conduction and advection can combine to drive lateral thaw. It is however challenging to quantify lateral thaw, and further investigation and instrumentation is needed including lateral temperature profiles, time-series geophysical data, and quantification of flow rates along the periphery of permafrost bodies. However, some extrapolations are possible from the available data, where the subsurface temperature data indicate that advection must play a key role in lateral permafrost degradation, especially adjacent to flowing fens. This also helps to explain the rapid thaw rates observed laterally as advection supplies warm water to maintain a thermal gradient laterally while the active layer is comparatively ineffective at maintaining a thermal gradient.

Evidence for this flow-enhanced thaw is shown in both the fen and also the winter road in Figure 4b. The observed thaw adjacent to the winter road (transects T1, T4 and T9 in Figure 1) spans a very wide range, though the mean temperature recorded there is much lower than in the permafrost-free wetland features. This is because the winter road traverses collapse scar wetlands and fens, and thaw rates are strongly affected by these wetlands as opposed to the road itself. The mean temperature data is taken from thermistors installed on the edge of a plateau bordering the winter road, hence the temperature near the freezing point. It is also relevant to note that this feature is unsaturated, and so the summer temperatures are much lower due to the limited thermal conductivity of dry peat.

Considering both processes of advection and conduction, the rapid lateral thaw rates are still somewhat higher than would be expected for completely frozen permafrost with a large vertical extent. The maximal expected thaw rate based on Equation 1 is 30 cm/year, and though it is challenging to quantify the flow rate in a fen, the thaw rates in Figure 4b indicate that the permafrost body that is thawing likely has a limited vertical extent, and was both exposed to degradation from above and potentially thaw from below, as well as the possibility that the permafrost is not completely frozen and thaw is already underway.

Finally, the rapid lateral permafrost thaw rate may in part be explained by the low ice content of the permafrost adjacent to wetlands. As shown in Figure 5a, the deep permafrost in many regions is isothermal at the freezing point depression. This indicates that phase change is likely occurring, and any change in enthalpy of the system is associated with latent heat as opposed to sensible heat. Unlike at the center of permafrost bodies, the edges of such bodies are continuously exposed to the thermal gradient driving thaw. This could result in loss in lateral extent of permafrost exceeding vertical losses because the ice content may be as low as 40% where peat plateaux border wetlands, as compared to the original ice content of 80% in a completely frozen profile. Anecdotal evidence from frost probe measurements taken in the field indicate that permafrost is “softer” near the edge of wetlands, and as depths approach 2 m. If thaw reaches a depth of 2 m, it is rare to find permafrost below that depth, except in linear disturbances on the landscape, such as winter roads and seismic lines where disturbance has driven disproportionate thaw from above.

5.3. Thaw From Below

When considering thaw from below, the first explanation is the geothermal heat flux, which is known to have a magnitude of approximately 0.08 W/m² at a depth of 50 m in this region (McClymont et al., 2013). This small flux would eventually degrade a permafrost body from below if it was not balanced by a net thermal loss from the surface. This heat flux could account for a maximal thaw rate of about 9.8 cm/year, assuming the permafrost is at the freezing point, none of the ground heat flux is consumed as sensible heat, and the permafrost loses no thermal energy over winter. In the absence of groundwater movement and lateral thermal gradients, it is expected that permafrost underlying a talik would degrade from below at this rate once it becomes isothermal as there is no mechanism for it to lose energy, resulting in an increase in internal energy. Given the increase in talik prevalence and a range of observed permafrost thickness of 5–13 m as

reported by (McClymont et al., 2013), this could result in total permafrost loss in the next 100 years due to this process alone.

In addition to the estimated thaw due to the geothermal heat flux, there is some evidence for additional groundwater-driven thaw in this field site. In Figure 5b, it is clear that the subsurface temperature at the edge of a degrading fen is increasing, whereas the subsurface temperature in a winter road not in proximity to a wetland is isothermal (Figure 5a). Though the isothermal condition of permafrost is likely indicative of phase change - the temperature is within the freezing point depression observed in this study site - it does not show evidence of a temperature gradient. The temperature at the edge of the fen however indicates a higher temperature at depth for most of the year, as seen in Figure 5b. This noticeable heat flux at depth (approximately 0.1 W/m^2) is not significantly greater than that expected due to geothermal heat flux, but does not preclude the possibility of a deep groundwater connection. This temperature profile also shows evidence for summer mixing (vertically) as the subsurface temperatures converge near their peak, but diverge in the cold winter months. Field observations of groundwater connections include upwelling and flooding of frozen wetlands in the early spring. This may provide further evidence that there is a groundwater source bringing energy to the system from below.

5.4. Talik Function

The cases above can be summarized by considering the red arrows in the conceptual diagram in Figure 2, which indicates the dominant thaw mechanism(s) in each landscape feature. Further to being indicative of the dominant thaw mechanisms, each of the talik configurations serves distinct functions in the discontinuous permafrost peatland environment. Talik function can be categorized as hydrologic, thermodynamic, or geophysical.

5.4.1. Hydrologic Function

Taliks predominantly serve as hydrologic storage features, or extensions of wetlands in the low relief discontinuous permafrost peatlands environment. In the cases of isolated taliks, there is rarely a hydraulic gradient to drive flow between the taliks and surrounding wetlands, and when there is, the storage features act to dampen the hydrologic response of the landscape. Based on water level measurements included in Figure S1, connected taliks seem to function as extensions of the wetland to which they are connected. In the case of flow-through taliks, their formation increases the hydrologic connectivity of the landscape as they rapidly erode permafrost allowing for quickflow, or shallow subsurface lateral flow between wetland features. There are two possible impacts of this increase in connectivity. The first is an increase in runoff ratio, where more of the water incident on the landscape is able to flow toward the basin outlet: the runoff ratio increased from 0.25 in the historic period to 0.43 for the recent period. This is supported by R. F. Connon et al. (2015), where there is evidence of increases in streamflow accompanying permafrost degradation, as seen in Figure 8, modified from R. F. Connon et al. (2021). Runoff ratio and streamflow data is presented from the Jean-Marie basin as it has a significantly longer period of hydrometric record than SC. It is situated directly adjacent to the Scotty Creek catchment, and has similar land cover though the basin area is an order of magnitude larger (1310 km^2 compared to 152 km^2). This change in runoff is not accompanied by a change in precipitation, and though it is possible that changes in vegetation may lead to altered runoff, these changes are linked to permafrost degradation and talik formation, as discussed in Section 5.4.3. The increase in runoff ratio could be due to changes in storage capacity in the wetland-dominated landscape, but these are also likely linked to the state of the permafrost. Other studies have also observed a trend in which talik formation increases the surface-water ground-water interaction such as McKenzie and Voss (2013), in which it is observed that groundwater flows drastically increase permafrost thaw rates.

The second major hydrologic impact of these subsurface flow pathways is on the winter quiescence of the peat plateaux-collapse scar wetland complexes. It is generally assumed that in the winter, flow in permafrost systems ceases as the active layer freezes down to the top of the permafrost table (Woo, 2012). However, once perennially thawed taliks exist in the landscape, they contribute to an increase in baseflow which is observed over the winter period, shown in the inset of Figure 8. It is therefore clear that the presence of taliks has the potential to significantly impact the seasonal runoff and baseflow regimes.

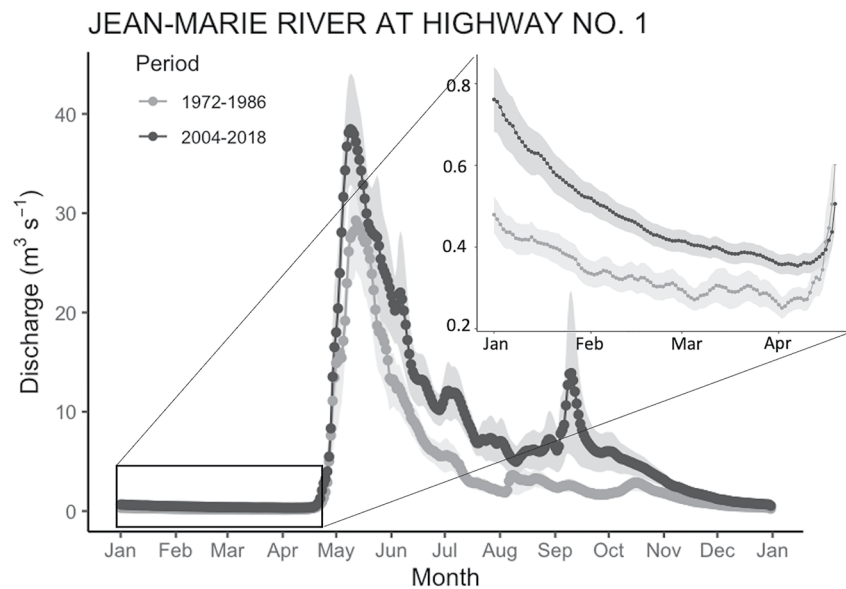


Figure 8. Increase in mean streamflow observed at the outlet of Jean-Marie River. This basin is adjacent to Scotty Creek with similar land cover classification, and a contributing area 10 times that of the Scotty Creek catchment (R. F. Connon et al., 2014). No statistically significant change in precipitation was observed over the documented period (R. F. Connon et al., 2021). Increase in baseflow observed especially over the winter months thought to be due to talik formation.

5.4.2. Thermodynamic Function

Most of the energy in this discontinuous permafrost landscape is associated with the sensible heat of liquid water, and so the thermodynamic function of taliks mirrors their hydrologic function. As such, isolated and connected taliks store energy, and accelerate permafrost thaw by preventing the over-winter cooling of the soil profile as discussed in Section 5.1.2. Though flow-through taliks may convey heat with the water that is transported through them, it is more likely that the heat stored in water flowing through them is conducted into the permafrost and active layer. This acts to accelerate thaw in these flow-through taliks, as well as alongside the edges of fens where lateral thaw progresses rapidly year-round. The presence of a talik often coincides with increased soil moisture and depressions formed due to subsidence, leading to the positive feedback cycle discussed in the introduction (Quinton & Baltzer, 2013).

5.4.3. Geophysical Function

In a geophysical sense, ground ice lends significant structure to the discontinuous permafrost peatlands environment. It is clear from the landscape that forested areas are generally limited to peat plateaux, which are underlain by permafrost. Once permafrost degradation takes place, subsidence causes the dry ground to meet the water table, flooding the roots of the canopy and resulting in the loss of the black spruce over-story (Baltzer et al., 2014). Subsidence is especially evident in permafrost adjacent to wetlands, and it is possible that thaw from below is causing this more rapid change in ground surface elevation. In some areas where permafrost has degraded and subsequent drainage has occurred, a tree canopy may return to the landscape, but it is unclear whether this is a stable condition, and if these treed environments are suited to future conditions (Disher et al., 2021; Haynes et al., 2021). The fact that permafrost loss results in landscape transitions points to the nonstationarity of this system, indicating that it is perhaps inappropriate to represent any given location in the landscape using a model with static land-cover classifications. A schematic of this change is presented in O. Carpino et al. (2021), in which a space-for-time approach is taken to consider the changes in discontinuous permafrost landscapes.

5.5. Nonstationarity

It is clear from the the results presented above that permafrost is changing rapidly at the SC, and in similar field sites across northern Canada (O. Carpino et al., 2021; O. A. Carpino et al., 2018). This change necessitates an evolving description of the landscape in order to track processes. A clear example of this rapid change is shown in Figure 7, where vertical and lateral thaw rates are presented in two flow-through talik sites. The similarities in both vertical and lateral permafrost degradation over the past four years are remarkable. This figure also highlights the fact that any one thaw mechanism is not acting independently - vertical and lateral thaw occur simultaneously and must both be represented to accurately predict permafrost degradation. Thus, Figure 2 may describe the predominant mechanism for thaw in each case, but not the exclusive mechanism.

Not only are thaw mechanisms acting simultaneously, but the data in Figure 7 indicate co-dependence of thaw rates. There are two notable changes in this figure, the first is when the thaw depth exceeds 70 cm, and both the vertical and lateral thaw rates increase notably. This may indicate the point at which a connected talik was formed allowing for advection to act alongside vertical conduction. A second tipping point can be identified when the plateau width is 15–20 m, and the rate of permafrost thaw again increases. This may indicate the action of lateral as well as vertical thaw processes and thaw from below. Additionally, as the talik thickens there is potential for active layer thinning as the thermal storage in the talik increases and counteracts the maximum refreeze depth. This was found in earlier work at SC, where the maximum depth of refreeze seems to increase with talik thickness (Devoie et al., 2019). We also note that once permafrost is not present in the soil column, there is potential for the geothermal heat flux to limit refreeze depth as well. Together, these effects require a dynamic modeling system that includes different thaw drivers at different stages in permafrost degradation. In order to accurately predict long-term changes in this system, models would need to incorporate potential for groundwater exchange, lateral and vertical thaw from above and below, as well as an ecological model to account for changes in surface vegetation and thus incoming energy. This discussion of nonstationarity focuses only on the state of the permafrost and its implications for thaw rates, but this is of course inextricably linked with climate drivers, which are evolving due to climate change.

5.6. Talik Evolution - Trajectory of Change

Figure 4 shows that the mean permafrost degradation rate across this landscape is positive. This indicates that permafrost at SC is in disequilibrium with the climate, and due to changes in climate this region is headed toward permafrost-free conditions. As presented in O. Carpino et al. (2021), there is a trajectory of change in which the formation of an isolated talik results from increased net radiation. The positive feedback driven by subsidence, canopy thinning, decreased albedo, and increased thermal conductivity causes talik expansion, leading to connection(s) with wetlands. Degradation continues, with the potential for advection along with conduction, and lateral thaw in addition to the vertical thaw. Plateaux are then expected to degrade, forming either collapse scar wetlands or fens. Evidence for collapse scar wetland capture, in which collapse scar wetlands expand until they become hydrologically indistinct, is presented in Haynes et al. (2018). This process eventually leads to landscape drying as it is shown here that widespread thaw has the potential result in increased hydrologic connectivity and landscape drainage resulting in the re-establishment of a tree canopy on a permafrost-free landscape (O. Carpino et al., 2021).

6. Conclusion

This study clarifies the role of various heat transfer mechanisms on the evolution of discontinuous permafrost under a range of conditions. It was found that vertical conduction is responsible for most of the thaw at the top of the permafrost table, while advection is needed to adequately represent thaw rates in flow-through taliks. This simplifies the model requirements for many situations, where 1-D conduction-only models are sufficient to represent isolated and connected talik features. Lateral thaw occurs at a rate about an order of magnitude greater than vertical thaw, and shows clear dependence on the movement of water in the subsurface. Deep subsurface temperatures provide evidence for thaw from below where the geothermal heat flux may be responsible for significant thinning of degrading permafrost bodies. The

temperature profiles of much of the discontinuous permafrost measured at SC are isothermal at the freezing point, indicating potential for partially frozen subsurface conditions where the pore ice is undergoing phase change. Though the processes governing permafrost thaw at specific sites have been distinguished here, the system is non-stationary, and thus different processes are expected to dominate permafrost thaw as the system changes. Not only is the behavior non-stationary, but it is also site-specific and variable in both space and time. Degradation generally follows a pattern of talik formation and evolution in which isolated taliks become connected, with a potential for flow-through, and then degrade entirely, merging with wetlands. An understanding of this trajectory is helpful not only in identifying stages of permafrost degradation in discontinuous permafrost peatlands, but also in selecting which governing processes and how many dimensions need to be represented in thermal and hydrologic models in order to adequately represent degrading permafrost. This work points to the value of long-term process-based observations in improving our understanding of permafrost systems, and highlights the need for integrated thermal, hydrological and ecological models to describe evolving permafrost systems.

Data Availability Statement

The data that support the findings of this study are openly available in the Wilfrid Laurier University Library archive (Devoie & Quinton, 2020): <https://doi.org/10.5683/SP2/J2KBPF> as well as from the Water Survey of Canada (Water Survey of Canada, 2020): https://wateroffice.ec.gc.ca/report/historical_e.html?stn=10FB005.

References

- Ackley, C., Tank, S. E., Haynes, K. M., Rezanezhad, F., McCarter, C., & Quinton, W. L. (2021). Coupled hydrological and geochemical impacts of wildfire in peatland-dominated regions of discontinuous permafrost. *The Science of the Total Environment*, 782, 146841. <https://doi.org/10.1016/j.scitotenv.2021.146841>
- Amiri, E. A., & Craig, J. R. (2019). Effect of soil thermal heterogeneity on permafrost evolution. *Cold Regions Engineering*, 492–499. <https://doi.org/10.1061/9780784482599.057>
- Baltzer, J. L., Veness, T., Chasmer, L. E., Sniderhan, A. E., & Quinton, W. L. (2014). Forests on thawing permafrost: Fragmentation, edge effects, and net forest loss. *Global Change Biology*, 20(3), 824–834. <https://doi.org/10.1111/gcb.12349>
- Bonnaventure, P. P., & Lamoureux, S. F. (2013). The active layer: A conceptual review of monitoring, modelling techniques and changes in a warming climate. *Progress in Physical Geography*, 37(3), 352–376. <https://doi.org/10.1177/2F0309133313478314>
- Carpino, O., Haynes, K., Connon, R., Craig, J., Devoie, E., & Quinton, W. (2021). Long-term climate-influenced land cover change in discontinuous permafrost peatland complexes. *Hydrology and Earth System Sciences*, 25(6), 3301–3317. <https://doi.org/10.5194/hess-25-3301-2021>
- Carpino, O. A., Berg, A. A., Quinton, W. L., & Adams, J. R. (2018). Climate change and permafrost thaw-induced boreal forest loss in north-western Canada. *Environmental Research Letters*, 13(8), 084018. <https://doi.org/10.1088/1748-9326/aad74e>
- Chasmer, L., Quinton, W., Hopkinson, C., Petrone, R., & Whittington, P. (2011). Vegetation canopy and radiation controls on permafrost plateau evolution within the discontinuous permafrost zone, Northwest Territories, Canada. *Permafrost and Periglacial Processes*, 22(3), 199. <https://doi.org/10.1002/ppp.724>
- Connon, R., Devoie, E., Hayashi, M., Veness, T., & Quinton, W. (2018). The influence of shallow taliks on permafrost thaw and active layer dynamics in subarctic Canada. *Journal of Geophysical Research: Earth Surface*, 123(2), 281–297. <https://doi.org/10.1002/2017JF004469>
- Connon, R. F., Chasmer, L., Haughton, E., Helbig, M., Hopkinson, C., Sonnentag, O., & Quinton, W. L. (2021). The implications of permafrost thaw and land cover change on snow water equivalent accumulation, melt and runoff in discontinuous permafrost peatlands. *Hydrological Processes*, 35(9), e14363. <https://doi.org/10.1002/hyp.14363>
- Connon, R. F., Quinton, W. L., Craig, J. R., Hanisch, J., & Sonnentag, O. (2015). The hydrology of interconnected bog complexes in discontinuous permafrost terrains. *Hydrological Processes*, 29(18), 3831–3847. <https://doi.org/10.1002/hyp.10604>
- Connon, R. F., Quinton, W. L., Craig, J. R., & Hayashi, M. (2014). Changing hydrologic connectivity due to permafrost thaw in the lower Liard River Valley, NWT, Canada. *Hydrological Processes*, 28(14), 4163–4178. <https://doi.org/10.1002/hyp.10206>
- Devoie, E. G., Connon, R. F., Craig, J. R., & Quinton, W. L. (2020). Subsurface flow measurements using passive flux meters in variably-saturated cold-regions landscapes. *Hydrological Processes*, 34, 4541–4546. <https://doi.org/10.1002/hyp.13900>
- Devoie, E. G., & Craig, J. R. (2020). A semianalytical interface model of soil freeze/thaw and permafrost evolution. *Water Resources Research*, 56(8), e2020WR027638. <https://doi.org/10.1029/2020WR027638>
- Devoie, E. G., Craig, J. R., Connon, R. F., & Quinton, W. L. (2019). Taliks: A tipping point in discontinuous permafrost degradation in peatlands. *Water Resources Research*, 55(11), 9838–9857. <https://doi.org/10.1029/2018WR024488>
- Devoie, E. G., & Quinton, W. L. (2020). *Talik function*. (Data collected at SCRS in support of talik function). <https://doi.org/10.5683/SP2/J2KBPF>
- Disher, B. S., Connon, R. F., Haynes, K. M., Hopkinson, C., & Quinton, W. L. (2021). The hydrology of treed wetlands in thawing discontinuous permafrost regions. *Ecohydrology*, 14, e2296. <https://doi.org/10.1002/eco.2296>
- Fourier, J. B. J. (1878). *The analytical theory of heat*. The University Press.
- Gordon, J., Quinton, W. L., Branfireun, B., & Olefeldt, D. (2016). Mercury and methylmercury biogeochemistry in a thawing permafrost wetland complex, Northwest Territories, Canada. *Hydrological Processes*, 30(20), 3627–3638. <https://doi.org/10.1002/hyp.10911>
- Hayashi, M., Goeller, N., Quinton, W. L., & Wright, N. (2007). A simple heat-conduction method for simulating the frost-table depth in hydrological models. *Hydrological Processes*, 21, 2610–2622. <https://doi.org/10.1002/hyp.6792>

Acknowledgments

We greatly appreciate the support from Gabriel Hould Gosselin, John Coughlin and Dirk J. Friesen in data collection and fieldwork, as well as Kristine Haynes in data processing. We gratefully acknowledge the support of the Dehcho First Nations, in particular, the Liidlii Kue First Nation and Jean Marie River First Nation. We also thank these communities for their long-standing support of the Scotty Creek Research Station. This work was funded by ArcticNet through their support of the Dehcho Collaborative on Permafrost, and by the Natural Sciences and Engineering Research Council of Canada. We also acknowledge the Canada Foundation for Innovation for providing funding for infrastructure critical to this study and the Northern Scientific Training Program for providing additional funding for this project. The valuable contributions to this work from the anonymous reviewers is also appreciated.

- Haynes, K. M., Connon, R. F., & Quinton, W. L. (2018). Permafrost thaw induced drying of wetlands at Scotty Creek, NWT, Canada. *Environmental Research Letters*, 13(11), 114001. <https://doi.org/10.1088/1748-9326/aae46c>
- Haynes, K. M., Smart, J., Disher, B., Carpino, O., & Quinton, W. L. (2021). The role of hummocks in re-establishing black spruce forest following permafrost thaw. *Ecohydrology*, 14, e2273. <https://doi.org/10.1002/eco.2273>
- Hipel, K. W., & McLeod, A. I. (1994). *Time series modelling of water resources and environmental systems*. Elsevier Science.
- Kneisel, C., Hauck, C., Fortier, B. R., & Moorman, B. (2008). Advances in geophysical methods for permafrost investigations. *Permafrost and Periglacial Processes*, 19(2), 1826–2178. <https://doi.org/10.1002/ppp.616>
- Lewkowicz, A. G., Etzelmüller, B., & Smith, S. L. (2011). Characteristics of discontinuous permafrost based on ground temperature measurements and electrical resistivity tomography. *Permafrost and Periglacial Processes*, 22(4), 320–342. <https://doi.org/10.1002/ppp.703>
- Loke, M. H., Acworth, I., & Dahlin, T. (2003). A comparison of smooth and blocky inversion methods in 2d electrical imaging surveys. *Exploration Geophysics*, 34(3), 182–187. <https://doi.org/10.1071/EG03182>
- McClymont, A., Hayashi, M., Bentley, L., & Christensen, B. (2013). Geophysical imaging and thermal modeling of subsurface morphology and thaw evolution of discontinuous permafrost. *Journal of Geophysical Research: Earth Surface*, 118, 1826–1837. <https://doi.org/10.1002/jgrf.20114>
- McKenzie, J. M., & Voss, C. I. (2013). Permafrost thaw in a nested groundwater-flow system. *Hydrogeology Journal*, 21(1), 299–316. <https://doi.org/10.1007/s10040-012-0942-3>
- O'Neill, H. B., Roy-Leveille, P., Lebedeva, L., & Ling, F. (2020). Recent advances (2010–2019) in the study of taliks. *Permafrost and Periglacial Processes*, 31(3), 346–357. <https://doi.org/10.1002/ppp.2050>
- Pörtner, H.-O., Roberts, D., Masson-Delmotte, V., Zhai, P., Tignor, M., Poloczanska, E., & Weyer, N. (2019). *IPCC, 2019: IPCC special report on the ocean and cryosphere in a changing climate*.
- Price, J. S., Cagampan, J., & Kellner, E. (2005). Assessment of peat compressibility: Is there an easy way? *Hydrological Processes: International Journal*, 19(17), 3469–3475. <https://doi.org/10.1002/hyp.6068>
- Quinton, W. L., & Baltzer, J. L. (2013). The active-layer hydrology of a peat plateau with thawing permafrost (Scotty Creek, Canada). *Hydrogeology Journal*, 21(1), 201–220. <https://doi.org/10.1007/s10040-012-0935-2>
- Quinton, W. L., Berg, A., Braverman, M., Carpino, O., Chasmer, L., Connon, R. F., et al. (2019). A synthesis of three decades of eco-hydrological research at Scotty Creek, NWT, Canada. *Hydrology and Earth System Sciences*, 23, 2015–2039. <https://doi.org/10.5194/hess-23-2015-2019>
- Quinton, W. L., Berg, A., Carpino, O., Connon, R. F., Craig, J. R., Devoie, É. G., & Johnson, E. (2017). Toward understanding the trajectory of hydrological change in the southern taiga plains, northeastern British Columbia and southwestern Northwest Territories. *Geoscience BC Summary of Activities*, Report 2018-4, pp. 77–86.
- Quinton, W. L., Hayashi, M., & Chasmer, L. (2009). Peatland hydrology of discontinuous permafrost in the Northwest Territories: Overview and synthesis. *Canadian Water Resources Journal*, 34(4), 311–328. <https://doi.org/10.4296/cwrj3404311>
- Quinton, W. L., Hayashi, M., & Pietroniro, A. (2003). Connectivity and storage functions of channel fens and flat bogs in northern basins. *Hydrological Processes*, 17(18), 3665–3684. <https://doi.org/10.1002/hyp.1369>
- Rezanezhad, F., Price, J. S., & Craig, J. R. (2012). The effects of dual porosity on transport and retardation in peat: A laboratory experiment. *Canadian Journal of Soil Science*, 92(5), 723–732. <https://doi.org/10.4141/cjss2011-050>
- Shiklomanov, N. I., Streletskiy, D. A., & Nelson, F. E. (2012). Northern hemisphere component of the global circumpolar active layer monitoring (CALM) program. In *Proc. 10th Int. Conf. on Permafrost* (Vol. 1, pp. 377–382).
- Sjöberg, Y., Coon, E., Sannel, A. B. K., Pannetier, R., Harp, D., Frampton, A., et al. (2016). Thermal effects of groundwater flow through subarctic fens: A case study based on field observations and numerical modeling. *Water Resources Research*, 52(3), 1591–1606. <https://doi.org/10.1002/2015WR017571>
- Walvoord, M. A., & Kurylyk, B. L. (2016). Hydrologic impacts of thawing permafrost: A review. *Vadose Zone Journal*, 15(6), 377–382. <https://doi.org/10.2136/vzj2016.01.0010>
- Walvoord, M. A., Voss, C. I., Ebel, B. A., & Minsley, B. J. (2019). Development of perennial thaw zones in boreal hillslopes enhances potential mobilization of permafrost carbon. *Environmental Research Letters*, 14(1), 015003. <https://doi.org/10.1088/1748-9326/aaf0cc>
- Water Survey of Canada. (2020). *Historical hydrometric data*. Retrieved from <https://wateroffice.ec.gc.ca>
- Way, R. G., Lewkowicz, A. G., & Zhang, Y. (2018). Characteristics and fate of isolated permafrost patches in coastal Labrador. *The Cryosphere*, 12(8), 2667–2688. <https://doi.org/10.5194/tc-12-2667-2018>
- Woo, M.-k. (2012). *Permafrost hydrology*. Springer Science & Business Media.
- Wright, N., Hayashi, M., & Quinton, W. L. (2009). Spatial and temporal variations in active layer thawing and their implication on runoff generation in peat-covered permafrost terrain. *Water Resources Research*, 45(5), W05414. <https://doi.org/10.1029/2008WR006880>